Effects of pore water chemical composition on the hydro-mechanical behavior of natural stiff clays

Xuan-Phu Nguyen, Yu-Jun Cui, Anh Minh A.M. Tang, Yongfeng Deng, Xiang-Ling Li, Laurent Wouters

Effects of pore water chemical composition on the hydro-mechanical behavior of natural stiff clays

X. P. Nguyen[1], Y. J. Cui[1], A. M. Tang[1], Y. F. Deng[2], X. L. Li[3], L. Wouters[4]

1. Ecole des Ponts ParisTech, Navier/CERMES, Marne-la-Vallée, France (phunguyenx@gmail.com)
2. Southeast University, Institute of Geotechnical Engineering, Transportation College, Nanjing, China
3. Euridice c/o SCK/CEN, Mol, Belgium (xli@sckcen.be)
4. ONDRAF, Belgium (l.wouters@nirond.be)

Corresponding author:
Prof. Yu-Jun CUI
Ecole des Ponts ParisTech
6-8 av. Blaise Pascal, Cité Descartes, Champs-sur-Marne
F-77455 MARNE LA VALLEE
France
Telephone: +33 1 64 15 35 50
Fax: +33 1 64 15 35 62
E-mail: yujun.cui@enpc.fr

Abstract: Boom Clay and Ypresian Clays have been considered as potential geological host formations for radioactive waste disposal in Belgium. Considering the significant differences in pore water chemical composition between several sites involving these two formations as well as the possible evolution of the chemical composition during the large lifespan of a radioactive waste disposal, it appeared important to investigate the effects of pore water chemical composition on the hydro-mechanical behaviors of these two potential host formations. In this study, these effects were investigated by carrying out specific œdometer tests. Different compositions were considered for this purpose: distilled water, synthetic site water, Sodium Chloride solutions at concentrations of 15 and 30 g/L. Clear effects of pore water chemical composition on the hydro-mechanical behavior were observed: increasing pore water salt concentration gave rise to (i) increase of œdometric modulus $E_{œd}$, permeability K and consolidation coefficient C_v ; and (ii) decrease of compression slope c'_c, swelling slope c'_s and secondary compression coefficient $C_{\alpha e}$, which is in agreement with the diffuse double layer theory and the clay particle aggregation as identified by microstructural analyses. Furthermore, the pore water chemical composition effects were found to be mineralogy, stress state and salt concentration dependent: (i) Ypresian Clays with higher smectite content showed clearer chemical effect on the coefficient of consolidation C_v; (ii) the chemical effects on compressibility and swelling capacity parameters were found to be attenuated with increasing vertical stress; and (iii) the increase of chemical effect with increasing pore water salinity was limited to a certain salt concentration. The competition between the physico-chemical and mechanical effects was identified: the pore water chemical composition effect is clear only in the low-stress range where the hydro-mechanical behavior is dominated by the physico-chemical effect.

Keywords: Boom Clay; Ypresian Clays; œdometer test; physico-chemical effect; hydro-mechanical behavior.

1. Introduction

Two clay formations, Boom and Ypresian, have been considered as potential geological host formations for high-level and/or long-lived radioactive waste disposal in Belgium. Several sites have been investigated, such as Mol and Essen for Boom Clay, Doel and Kallo for Ypresian Clays. Significant variations in pore water salinity between these sites have been reported (De Craen et al., 2004, 2006; van Marcke and Laenen, 2005; van Marcke, 2009). In addition, the pore water salinity at each site may also evolve at the time scale of radioactive waste disposal. This can substantially affect the hydro-mechanical behavior of the host formations. Therefore, it is essential to evaluate the sensitivity of the hydro-mechanical behavior of the host formations to changes in pore water chemical composition.

Most of studies involving chemical effects on the hydro-mechanical behaviors of soils were conducted on reconstituted soils and natural soft soils. Various preparation methods were developed in the laboratory for this purpose: i) mixing the soil powder with a desired solution; ii) immersing a soil sample in a solution; iii) percolating a soil sample by a solution. Di Maio and Fenelli (1994), Di Maio (1998, 1996), Di Maio et al. (2004), Gajo and Loret (2007), Loret et al., (2002), Rao and Thyagaraj (2007), Yukselen-Aksoy et al. (2008) showed significant effects of pore water saline concentration on the hydro-mechanical behavior of reconstituted expansive clays with wide ranges of concentrations: i) changes in salt concentration and ion-type result in reversible or irreversible volume changes of soil, mainly by osmotic consolidation or osmotic

swelling; ii) increasing vertical stress reduces the extent of chemically-induced volume change; and iii) the compressibility and swelling capacity are reduced by increasing salt concentration. These effects have commonly been explained with the Guy-Chapman's theory of diffuse double layer (Mitchell and Soga, 2005).

For the non-active clays, Chen et al. (2000), Olson and Mesri (1970), Sridharan and Rao (1973), Wahid et al. (2011a, 2011b) found that they are relatively inert with respect to changes in pore water salt concentration, but sensitive to changes in *pH* (due to the mineral dissolution and the degradation of particle edges) and dielectric constant (due to the van de Waals attractive force).

For the natural stiff clays, the pore water chemical composition effect has been rarely studied. Swelling tests were carried out on the Callovo-Oxfordian claystone with distilled water and several saline solutions under different stress levels by Daupley (1997) and Wakim (2005). It was observed that the higher the salt concentration, the lower the swelling capacity. The same conclusion was drawn by Coll et al. (2008) for natural Boom Clay (Mol site, 223 m depth). For unsaturated compacted Boom Clay, Mokni et al. (2012) observed a significant effect of salt concentration on the water retention property but a negligible effect on the compressibility. On the other hand, only a slight pore water chemical composition effect was identified by Deng et al. (2011a) on the hydro-mechanical behavior of Boom Clay at Essen (227 m depth). The reason is probably the slight difference between the two solutions considered, distilled water and synthetic Boom Clay water (SBCW – water prepared from salts' powder having similar chemistry as *in situ* pore water), as well as the limited amount of smectite in Boom Clay. Comparison with reconstituted expansive clays shows that natural stiff clays respond to changes in pore water salt concentration in the same fashion, but to a lesser extent. This is probably due to the fact that only the active clays fraction (smectite for example) in natural stiff clays is sensitive to changes in

pore water chemical composition. Moreover, the natural clay structure, *i.e.* particle arrangement and inter-particle bonding (Burland, 1990), developed at great depths since several millions years may also attenuate the effect of pore water salinity changes.

In the present work, the effects of pore water chemical composition on the swelling capacity, compressibility, permeability, consolidation and secondary compression/swelling of Boom Clay and Ypresian Clays were investigated by means of specific œdometer tests. Intact samples with Sodium Chloride solutions at 15 and 30 g/L-concentrations were tested. Data from two similar tests on Boom Clay with distilled water and SBCW (Deng et al., 2011a; Nguyen, 2013) will be incorporated for further analysis. Microstructure analyses were also performed on samples in both intact and after-test states, providing further insight into the mechanisms of chemical impact on the hydro-mechanical behavior of natural stiff clays.

2. Materials and methods

2.1. Boom Clay

Boom formation was deposited in the Rupelian stage, about 36-30 millions years ago, in the Southern part of the North Sea basin (ONDRAF, 2001). In Belgium, Boom Clay is located in the Northeast, in the Campine region. This Tertiary formation outcrops near the Antwerpen city, gently dips and thickens toward the Northeast direction. It corresponds to a marine sediment sequence of silty clays and clayey silts, and is subdivided into four members from bottom to top with depths at the Essen site: Belsele-Waas (260 - 280 m), Terhagen (237 - 260 m), Putte (200 - 237 m), and Boeretang (154 - 200 m). The soil studied (BE83) was vertically cored in a borehole at the Essen site, from 226.65 m to 227.75 m depth, in the lower part of Putte member. This member is the most clayey one, dark gray in color, rich in organic matters and with low

carbonates content (ONDRAF, 2001). Note that the underground research laboratory (URL) HADES constructed at the Mol site is also situated in this member.

The mineralogical composition of Boom Clay BE83 (Deng et al., 2011b) was determined by X-ray diffractometry and presented in Table 1 for the bulk mass and in Table 2 for the clay-size fraction (< 2 μm). It can be observed that the Boom Clay mineralogy is dominated by non-clay minerals (60 % in bulk mass), and smectite represents about 20 % of the clay-size fraction.

The particle-size distribution curve of Boom Clay (Deng et al., 2011c) by hydrometer methods following the French standard (AFNOR, 1992) is shown in Figure 1. The results of Boom Clay at Mol at 223 m depth (BM223) from Baldi et al. (1988), Coll (2005), Lima (2011) and Romero (1999) are also presented. It appears that Boom Clay at Mol and Essen has similar particle-size distribution.

The physical and index properties of Boom Clay are shown in Table 3. It can be observed that according to ASTM (2006), Boom Clay is highly plastic with a liquid limit LL = 67.2 and a plastic limit PI =34.7. Its carbonate content is quite low, and at its initial state it is fully saturated with $S_{r0} \approx 100$ %.

Table 4 gives the synthetic pore water chemical composition of Boom Clay (De Craen et al., 2006), indicating that Na^+ is the main cation.

2.2. Ypresian Clays

Ypresian Clays were formed by marine deposition during the Ypresian period (55 - 49.6 Ma). It comprises four members, from bottom to top with depths at the Kallo site: Orchies (380 - 400 m), Roubaix (311 - 380 m), Aalbeke (303 - 311 m) and Kortemark (289 - 303 m). The clays sequence roughly corresponds to the London clay in the Southeast of England, the basal part of

the Dutch Dongen formation and the Flandres clay in Northern France (van Marcke and Laenen, 2005). The soil studied (YK74) was also taken from a cored borehole at the Kallo site at a depth of 361.81 – 362.60 m in the lower part of the Roubaix member (Cammaer et al., 2009).

The mineralogical composition of Ypresian Clays YK74 by X-ray diffractometry is presented in Table 1 for the bulk mass and in Table 2 for the clay-size fraction (Vandenberghe, 2011). Non-clay minerals represent only 43 % in the bulk mass while the smectite content is about the two-third of the clay-size fraction and one-third of the bulk mass.

The particle-size distribution curve of Ypresian Clays is shown in Figure 1 (Vandenberghe, 2011). Compared to Boom Clay, Ypresian Clays are finer.

The physical and index properties of Ypresian Clays are shown in Table 3. According to ASTM (2006), they are also highly plastic with a liquid limit LL = 136.6, a plastic limit PI = 100.5 and a blue methylene value VBS = 13.1 g/100g (twice the value of BE83). The carbonate content is low. At their initial state, Ypresian Clays are slightly unsaturated with $S_{r0} < 95$ %.

The synthetic pore water chemical composition of Ypresian Clays is shown Table 4 (van Marcke, 2009). Na^+ is also observed as the main cation with a concentration (0.13 M) about twice that of Boom Clay (0.07 M). Note that the *in situ* pore water chemical compositions of Boom Clay at Mol and Essen are also different (De Craen et al., 2006). Note also that the pore water salinities of Ypresian Clays and Boom Clay are still respectively 4 and 7 times lower than that of the North Sea (about 35 g/L - 0.6 M NaCl).

2.3. Sample preparation, test procedure and program

Oedometer tests were conducted on soil samples of 50 mm diameter and 20 mm height. These samples were hand-trimmed from cores (YK74 and BE83) having the dimensions of 1.0 m in length and 100 mm in diameter.

Figure 2 presents the test procedure adopted in this study. After installing the soil sample in the œdometer cell, step loading (A-B) up to the *in situ* vertical effective stress (σ'_{v0} = 2.4 MPa for BE83 and 3.2 MPa for YK74) was carried out without putting the sample in contact with water in order to avoid soil swelling which would affect the soil microstructure and thereby the soil hydro-mechanical behavior (Delage et al., 2007; Deng et al., 2011a, 2011b, 2011c, 2012).

After application of σ'_{v0}, the bottom porous stone and the drainage system were filled with synthetic water (B-C). A controller of pressure/volume (CPV) was then used to flush synthetic water out of the bottom porous stone and the drainage system via the other inlet by a desired solution (distilled water, synthetic water, NaCl at 15 or 30 g/L-concentrations). This solution was then injected through the bottom porous stone into the soil sample (C-D). The injection pressure was raised in steps to 1 MPa and then kept constant until the injected volume of the desired solution was more than twice the sample pore volume. This volume criterion was expected to be appropriate for fully replacing the initial pore water of the soil sample by the desired solution. Based on the flow monitoring during this stage, the hydraulic conductivity and then the intrinsic permeability were determined by the constant-head method. After stepwise decreasing the injection pressure to zero (D-I), the CPV was replaced by a container filled with the same solution in order to keep the sample saturated.

Unloading from σ'_{v0} to 0.05 MPa (I-II), reloading from 0.05 MPa to 3.2 MPa (II-III) and unloading again to 0.05 MPa (III-IV) were finally performed in steps. The French standard (AFNOR, 1997) was applied for the volume change criterion: the volume change was considered as steady when the vertical strain rate was lower than 5.10^{-4}/8 h.

Table 5 summarizes the four tests (BO3, BO4, YO1 and YO2) carried out in this study. Note that two tests (BO1, BO2) conducted by Deng et al. (2011a) and Nguyen (2013) are also reported in this table. The initial void ratio e_0 and initial degree of saturation S_{r0} for each sample are also given. Scanning Electron Microscopic (SEM) and Mercury Intrusion Porosimetry (MIP) were carried out on freeze-dried (Delage et al., 2006) Boom Clay samples in both the intact and after-test states. These analyses were unfortunately not performed on intact Ypresian Clays sample because the sample was fissured. For convenience, while analyzing the microstructure results, the after-test samples are also termed by the name of the corresponding test. For instance, BO4 sample means the sample taken at the end of test BO4 (Boom Clay with NaCl solution at 30 g/L-concentration) and then freeze-dried.

3. Results

3.1. Typical results and parameters definition

Figure 3 presents a typical compression curve obtained from test BO4. The initial loading up to the *in situ* vertical effective stress σ'_{v0} = 2.4 MPa without putting soil sample in contact with water resulted in a compression from e_0 = 0.723 to e = 0.619 with a slope-changing point at σ_v = 1.6 MPa. The degree of saturation S_r (estimated for each step from the measured volume changes assuming a constant water content $w = w_0$) reached 100% at the end of this initial loading for all the tests. Le et al. (2011) also observed that Boom Clay at Mol at 223m depth (BM223) samples

reached fully saturated state under a vertical stress σ_v of 1.6 MPa (indicated by the measured suction equal to zero).

The results during soaking with SBCW and during injection of NaCl solution at 30 g/L-concentration are presented in the inset diagram. It can be observed that soaking induced negligible compression (Δe = 0.619 - 0.617) while injection of NaCl at 30 g/L-concentration produced a slightly higher compression (Δe = 0.617 - 0.610).

For further analysis of the chemical effect during the injection stage, volume changes during the last loading step from σ_v = 1.6 - 2.4 MPa before soaking, during soaking with SBCW and during injection of NaCl solution at 30 g/L-concentration are detailed in Figure 4. It is observed that the volume change during soaking followed the same slope as the secondary compression in the last loading step, indicating a continuous creep behavior without any chemical effect. During injection, several mechanisms are involved: (i) unloading due to the application of injection pressure $P_{CPV\max}$ = 1MPa; (ii) reloading due to the removal of injection pressure; (iii) creep; and (iv) chemical effects due to changes in pore water chemical composition. The total compression identified in Figure 3 is the combined effect of all the four mechanisms.

Figure 5a zooms the circled part in Figure 4. The injection pressure variation is shown in Figure 5b. Considering that the maximum value of injection pressure $P_{CPV\max}$ = 1MPa is much lower than the *in situ* vertical effective stresses σ'_{v0} = 2.4 and 3.2 MPa for Boom Clay and Ypresian Clays, respectively, the unloading and reloading during the application and the removal of injection pressure are rather in the elastic zone where the volume change induced can be assumed to be recoverable. Thereby, the total void ratio change during this stage is related to creep and chemical effects only:

$$\Delta e_{inj} = \Delta e_{C\alpha} + \Delta e_{Ch}$$

with $\Delta e_{C\alpha} = -C_{\alpha e}\Delta \log t_{inj}$. Note that $\Delta \log t_{inj} = \log(t_2/t_1)$ is the difference in logarithm of time at the end t_2 and at the beginning t_1 of the injection which are counted since the beginning of the last loading up to σ'_{v0} (Figure 5). The chemically-induced void ratio change Δe_{Ch} can therefore be deduced from the total void ratio change Δe_{inj} and the creep-induced void ratio change $\Delta e_{C\alpha}$.

The subsequent unloading, with NaCl solution at 30 g/L-concentration as "new" pore water, from σ'_{v0} = 2.4 MPa (I) to 0.05 MPa (II) gave rise to significant swell: the void ratio e reached a value larger than its initial one (e_0 = 0.723). The reloading path (II-III) formed a hysteretic loop with the unloading path (I-II). The second unloading path (III-IV) was quite similar to the first one (I-II).

From the compression curve, the compression slope c'_c and the swelling slope c'_s were determined for each loading step. The consolidation curve of each loading step was used to determine the consolidation coefficient C_v following the Casagrande method ($C_v = 0.197H^2/t_{50}$ where H is the drainage length; t_{50} is the time corresponding to 50% of consolidation degree), the hydraulic conductivity k ($k = C_v\rho_f g/E_{\text{œd}}$; where ρ_f is the unit mass of fluid; g is the acceleration due to gravity; $E_{\text{œd}}$ is the œdometric modulus) and intrinsic permeability K ($K = k\mu/\rho_f g$ where μ is the fluid dynamic viscosity). The coefficient of secondary compression/swelling $C_{\alpha e}$ defined as the corresponding slope $-\Delta e/\Delta \log t$ of the consolidation curve was also determined.

3.2. Volume change during solution injection

The chemically-induced volume change $\Delta\varepsilon_{vCh}$ was plotted versus the pore water Na^+ concentration in Figure 6. It appears that for Boom Clay, injecting distilled water induced soil swelling while injecting NaCl solution at 30 g/L-concentration induced soil compression.

Moreover, the higher the pore water Na^+ concentration, the higher the chemically-induced compression. For Ypresian Clays, injecting NaCl solution at 15 g/L-concentration caused soil swelling while injecting NaCl solution at 30g/L-concentration caused soil compression. Furthermore, a linear relationship was observed between the chemically-induced volume change and the pore water Na^+ concentration for both Boom Clay and Ypresian Clays, the two relationships being parallel.

3.3. Compressibility and swelling behavior

Figure 7 and Figure 8 show the compression slope c'_c, swelling slope c'_s and œdometric modulus $E_{œd}$ of each loading/unloading step versus the mean vertical stress σ_v. As the second unloading (III-IV) curve is similar to the first one (I-II), only the results of unloading I-II and reloading II-III are presented in these figures.

For Boom Clay, a clear influence of pore water salt concentration on the compression and swelling behavior was identified. The sample with distilled water (test BO1) showed the largest c'_c and c'_s values. These values decreased in the order of samples with SBCW (test BO2), NaCl solution at 15 and 30 g/L-concentrations (tests BO3 and BO4). The highest $E_{œd}$ was found for the samples with NaCl solution, and followed by those for the samples with SBCW and distilled water.

On the other hand, the influence of pore water salt concentration decreased as the differences between the curves was reduced with increasing vertical stress σ_v (from $\sigma_v \approx 0.5$ MPa for the compression index c'_c). Furthermore, it is observed that the differences in c'_c, c'_s and $E_{œd}$ between the samples with NaCl solution at 15 and 30 g/L-concentrations are negligible with respect to those between the samples with distilled water and SBCW, and between the samples

with SBCW and NaCl solution at 15 g/L-concentration. For Ypresian Clays, only the NaCl solution at 15 and 30 g/L-concentrations were considered, and the differences in c'_c, c'_s and $E_{\alpha d}$ between the two corresponding samples were not clear.

The consolidation coefficient C_v for each loading step during reloading path II-III is shown in Figure 9 versus the mean void ratio e and the mean vertical stress σ_v. It is observed that C_v decreased with compression (increasing σ_v, decreasing e) and then increased again. A clear chemical effect was observed for both soils as C_v increased with increasing pore water Na^+ concentration. At a given void ratio or vertical stress, the difference in C_v between Ypresian Clays samples with NaCl solution at 15 and 30 g/L-concentrations is higher than for Boom Clays samples.

The variations of the coefficient of secondary compression/swelling $C_{\alpha e}$ with void ratio e at the end of each step is shown in Figure 10. As $C_{\alpha e} = -\Delta e/\Delta \log t$, it is positive during loading and negative during unloading. A clear pore water chemical effect was observed for Boom Clay upon reloading (II-III): the higher the salt concentration, the lower the value of $C_{\alpha e}$ at a given void ratio. Moreover, the chemical effect was negligible at (i) low void ratio e (high vertical stress σ_v) and increased with increasing e (decreasing σ_v); (ii) high concentration and increased with decreasing concentration. However, the chemical effect on $C_{\alpha e}$ upon unloading was not clear.

The correlations between the coefficient of secondary compression $C_{\alpha e}$ and compression slope c'_c and between the coefficient of secondary swelling $C_{\alpha e}$ and swelling slope c'_s are shown in Figure 11. A linear relationship between $C_{\alpha e}$ and c'_c was attempted: $C_{\alpha e}/c'_c = 0.024$ for Boom Clay and 0.015 for Ypresian Clays, while a bi-linear relationship between $C_{\alpha e}$ and c'_s was verified. The chemical effect on these correlations was not clear.

3.4. Permeability

The intrinsic permeability K measured at the end of injection phase by the constant-head method and that determined by back-analysis using the consolidation curve of each reloading step (phase II-III) are shown in Figure 12 in a logarithmic scale as function of void ratio e. Linear relationships were obtained in this semi-logarithmical plane for Boom Clay and Ypresian Clays. Moreover, these relationships are parallel for each clay. Noticeable chemical effect was identified for both soils: the sample with higher pore water Na^+ concentration showed higher K, even though the difference between Boom Clay samples with distilled water and SBCW was not clear.

3.5. Microstructure observation

Figure 13 and Figure 14 show the MIP results for Boom Clay and Ypresian Clays, respectively. The intruded mercury void ratio e_m is defined as the ratio of mercury intrusion volume V_m to soil solid volume V_s. Note that the MIP technique can only cover a limited range of pore size, from 300 to 0.005 µm in apparent mercury entrance diameter D (corresponding to a pressure range from 0.1 to 200 MPa).

Intact Boom Clay showed mono-modal pore-size distribution (Figure 13b) with a dominant pore size around D = 0.15 µm - meso-pore following Romero (1999). After "replacing" the *in situ* pore water by NaCl solution at 15 (test BO3) or 30 g/L-concentrations (test BO4) and applying an unloading-reloading-unloading path under low vertical stresses ($0.05 \leq \sigma_v \leq 3.2$ MPa), the pore size distributions became more or less bi-modal with creation of a population of micro-pore around D = 0.06 µm, the population of meso-pore being at D = 0.25 µm that was slightly larger than the initial one. It appears also that under chemical and mechanical loadings (i) the pores

smaller than D = 0.06 μm were not affected; (ii) the density of intermediate pores ($0.06 \leq D \leq 0.2$ μm) was reduced and (iii) the density of larger pores ($D \geq 0.3$ μm) was increased. It is also observed that the density of the meso-pore population of BO4 sample (with NaCl solution at 30 g/L-concentration) is higher than that of BO3 (with NaCl solution at 15 g/L-concentration). Note that the populations appeared around D = 100 μm may correspond to macro-fissures created during sample preparation.

YO1 and YO2 samples with NaCl solution at 15 and 30 g/L-concentrations, respectively, show dominant micro-pores of 0.10 μm diameter. This dominant pore size is significantly smaller than that of the meso-pore populations of BO3 and BO4 samples.

Figure 15 and Figure 16 show the SEM photos for Boom Clay and Ypresian Clays, respectively, on the section perpendicular to the bedding plane marked by black lines. On the left side are the photos in dimensions of 125×100 μm, except for YO2 with dimensions of 250×200 μm. These figures were then zoomed to reach dimensions of 25×20 μm, except for YO2 with dimensions of 62.5×50 μm, on the right side. Well-developed preferential alignments of clay particles in the direction parallel to the bedding plane for both Boom Clay and Ypresian Clays were observed.

Comparing SEM photos of intact and BO3-4 samples shows that more clay aggregates were formed with a diameter around 10 μm in BO3-4 sample. Clay particles seemed to be thicker as a result of more stacked-up clay layers, and large inter-particle pores and small intra-particle ones were formed. Boom Clay after test became less dispersed as compared with its initial microstructure. Some connected pores of 1 μm diameter in Boom Clay (Figure 15c, d, e, f) and 2-5 μm in Ypresian Clays (Figure 16) were identified.

4. Discussion

4.1. Pore water changes during the injection phase

During the injection phase, the chemically-induced swelling by distilled water (test BO1), compressions by NaCl solutions at 15 (test BO3) and 30 g/L-concentrations (test BO4) for Boom Clay, and also compression by NaCl solution at 30 g/L-concentration (test YO2) for Ypresian Clays are in agreement with the common observations in terms of pore water salt concentration effects on the volume change behavior of active clays (Castellanos et al., 2008; Di Maio, 1996; Musso et al., 2013). These volume changes can be considered as osmotic swelling/consolidation as described by the diffuse double layer theory (Chapman, 1913; Gouy, 1910) or as osmotic suction changes $\Delta\pi$: as the salt concentration increases, the double layer thickness decreases and the osmotic suction π increases, leading to shrinkage of clay particles and hence volume change in the macroscopic level. However, the chemically-induced swells observed on Boom Clay sample with SBCW and Ypresian Clays sample with NaCl solution at 15 g/L-concentration suggest that other mechanisms are involved in this "chemically-induced" volume change. Further studies are then needed to clarify this point.

4.2. Compressibility and swelling capacity

In general, the hydro-mechanical behavior of clays is governed by the competing physico-chemical and mechanical effects (Cui et al., 2002, Le et al., 2011). The term "mechanical" refers to particles interactions through their direct contacts, while the term "physico-chemical" denotes interactions through the diffuse double layer (Robinson and Allam, 1998). Thus, for each loading or unloading path, there is a threshold stress σ_s dividing the compression curve into two zones, each one being governed by one effect (Figure 17): (i) upon unloading, when the external stress

is higher than the repulsive force related to the soil particles-water interaction (physico-chemical effect) or $\sigma_v > \sigma_{s1}$ for I-II path or σ_{s3} for III-IV path, low swelling volume change occurs; otherwise ($\sigma_v < \sigma_{s1}$ or σ_{s3}), higher swelling volume change can be expected; (ii) upon reloading, when the external stress is lower than the matric suction related to the physico-chemical effect ($\sigma_v < \sigma_{s2}$), this external stress is balanced by the repulsive force, leading to a small volume decrease; on the contrary, when the external stress becomes higher ($\sigma_v > \sigma_{s2}$), the mechanical effect becomes dominant giving rise to larger volume decrease (Cui et al., 2013; Nguyen, 2013). For Boom Clay and Ypresian Clays, the values of threshold stress σ_s are practically similar, estimated at about $\sigma_{s1} \approx \sigma_{s3} \approx 1.5$ MPa upon unloading and $\sigma_{s2} \approx 0.5$ MPa upon reloading (Nguyen, 2013). .

Deng et al. (2012) investigated the secondary compression behavior of Boom Clay and also observed a linear relationship between $C_{\alpha e}$ and c'_c, and a bi-linear relationship between $C_{\alpha e}$ and c'_s. These authors also related this bi-linearity to the competition between two mechanisms: mechanically dominated rebounding and physico-chemically dominated swelling. The linearity during reloading was however explained by the mechanical effect that is supposed to be the only governing mechanism. If we admit the previous interpretations, a bi-linearity between $C_{\alpha e}$ and c'_c should also be obtained, instead of linearity. The linear relationship between $C_{\alpha e}$ and c'_c obtained during the reloading path in Deng et al. (2012) and in this study could be explained by lack of some $C_{\alpha e}$ values corresponding to the first reloading steps under $\sigma_v < \sigma_{s2} \approx 0.5$ MPa where hydro-mechanical behavior is expected to be governed by the physico-chemical effect.

Robinson and Allam (1998) discussed the mechanical and physico-chemical effects on the consolidation coefficient C_v, and concluded that the increase of C_v with increasing σ_v is due to

the dominance of mechanical effect while the decrease of C_v is related to the increasing physico-chemical effect. This is consistent with the variations of C_v shown in Figure 9. On the other hand, it has been commonly observed that (i) C_v decreases with increasing liquid limit *LL* (Carrier, 1985; Raju et al., 1995; Robinson and Allam, 1998; Sridharan and Nagaraj, 2004); and (ii) *LL* increases with decreasing salt concentration (Di Maio, 1996; Gajo and Maines, 2007). This is also consistent with the results obtained in this study: the higher the pore water salt concentration, the higher the consolidation coefficient C_v.

It was observed in this study that the higher the pore water salt concentration, the higher the values of œdometer modulus $E_{œd}$ and coefficient of consolidation C_v, the lower the values of compression/swelling slope c'_c/c'_s and secondary compression coefficient $C_{œe}$. This chemical effect was attenuated with increasing vertical stress σ_v. This is in agreement with the previous results on both natural clays (Deng et al., 2011a; Wakim, 2005) and reconstituted swelling clays (Di Maio and Fenelli, 1994; Di Maio, 1996; Di Maio et al., 2004; Rao and Thyagaraj, 2007).

Basically, the pore water chemical composition effect should be more pronounced in the stress range where physico-chemical effects dominate. Indeed, when considering the chemical effects on soil compressibility and swelling capacity upon unloading (I-II and III-IV), it is observed that the variations of these parameters with different "new" pore waters are similar (the curves are parallel) until the threshold stress $\sigma_{s1} \approx 1.5$ MPa (Figure 17). Below the values of threshold stress σ_s, the curves start to have different slopes, increasing thereby the difference between the parameters with different "new" pore waters. Upon reloading (II-III), when the vertical stress was still below the threshold stress $\sigma_v < \sigma_{s2} \approx 0.5$ MPa, the difference between the parameters with different "new" pore waters are large while beyond the threshold σ_s, the gap is reduced with the curves approaching each other and become parallel again. This illustrates again that the pore

water chemical composition effects exhibit mainly in the stress range where the hydro-mechanical behaviour is dominated by physico-chemical effects.

It was found on Boom Clay that the increase of chemical effect with increasing pore water salinity was limited to a certain salt concentration. This observation was also reported in Di Maio et al. (2004) for several reconstituted clays of different smectite contents. Di Maio et al. (2004) also observed that the stabilizing concentration for a more expansive soil is lower. Thereby, the chemical effects on Ypresian Clays (containing higher smectite) should be stabilized at a lower pore water salt concentration than on Boom Clay. This is confirmed by that fact that the differences in $E_{\alpha d}$, c'_c, c'_s, and $C_{\alpha e}$ of Ypresian Clays between NaCl solution at 15 and 30 g/L-concentrations were found to be negligible.

4.3. Permeability

In the phase of *in situ* pore water replacement, it was observed that the higher the salt solution concentration, the higher the soil compression, and also the higher intrinsic permeability. Because, in general, permeability decreases with decrease of void ratio, the increased permeability must be due to other factors involved in this process.

Fernandez and Quigley (1985), Cui et al. (2003), while respectively studying a natural clay and the compacted Jossigny silt with distilled water and non-polar fluids, observed the importance of percolating fluid dielectric constant *D*: significant aggregation was observed with lower fluid dielectric constant, that led to a drastic increase in permeability. This is consistent with the results obtained in the present study because according to Wang and Anderko (2001), the dielectric constant *D* decreases in the order of distilled water, SBCW, NaCl solution at 15 and 30 g/L-concentrations, and this is also the increasing order of measured permeability.

On the other hand, previous works on FEBEX bentonite (Castellanos et al., 2008), MX-80 bentonite (Karnland et al., 1992; Villar, 2005), Na-Montmorillonite-sand mixtures (Studds et al., 1998), compacted Montmorillonite and Illite (Rolfe and Aylmore, 1977) and Friedland Ton clay - a natural clay with 45 % smectite (Push, 2001) also evidenced a clear increase in hydraulic conductivity with the increasing saline concentration of permeating fluid. Following Castellanos et al. (2008), several mechanisms can be involved, such as (i) modification of pore size distribution resulting from clay matrix swelling, and (ii) variations of water molecule mobility associated with exchangeable cations adsorbed on the clay sheet surfaces or in the diffuse double layer. Consequently, when the pore water salt concentration increases, there is reduction in the swelling capacity of clay particles, thus increasing large flow channel (inter-aggregate) size, causing permeability increase. On the contrary, any decrease in pore water salt concentration produces higher development of diffuse edouble layer, causing a decrease in permeability as a result of the decrease of the size of large flow channels.

The explanations above lead to the same conclusion in terms of microstructure changes: the size of large pores is increased by clay aggregation due to the pore water salt concentration increase, and the soil permeability is increased. After percolation, the influence of pore water salt concentration on permeability remained the same upon unloading-reloading-unloading: the higher the salt concentration, the higher the permeability. Moreover, the same slope of e – log$K$ curves was observed for each soil with different pore water chemical compositions, suggesting that the chemical effect on permeability was not affected by the vertical stress within the range considered. This means that the microstructure changes upon percolation can be considered as preserved during the unloading-reloading-unloading paths (I-II-III-IV). In other words, clay aggregation due to percolating NaCl solution at 15 and 30 g/L-concentrations (higher than the *in*

situ pore water salinity) was preserved until the end of the tests. The microstructure analyses by MIP and SEM confirmed this conclusion (see Figures 13-16).

5. Conclusions

The pore water salt concentration effects on the behaviors of natural Boom Clay and Ypresian Clays were investigated in terms of volume change, compressibility, swelling capacity, consolidation, creep and permeability. The results allow the following conclusions to be drawn:

(1) Percolation of a higher salt concentration solution induced soil compression (osmotic consolidation) while percolation of distilled water resulted in soil swelling (osmotic swelling); this is in agreement with the diffuse double layer theory;

(2) The higher the pore water salt concentration, the higher the œdometric modulus $E_{œd}$ and the coefficient of consolidation C_v, the lower the compression/swelling slope c'_c/c'_s and the secondary compression coefficient $C_{æ}$; this is also in agreement with the diffuse double layer theory;

(3) A higher chemical effect on the coefficient of consolidation C_v was identified for Ypresian Clays that have a higher smectite content than Boom Clay;

(4) The higher the pore water salt concentration, the higher the intrinsic permeability K due to the microstructure changes by clay aggregation - larger flow channels are formed as observed in the MIP and SEM analyses;

(5) The chemical effect on permeability was observed to be independent of vertical stress as the chemically-induced microstructure changes were preserved under mechanical loading;

(6) The pore water chemical composition effects on the compressibility and swelling capacity parameters were attenuated with increasing vertical stress σ_v upon loading/ unloading; bi-linear relationships between $C_{\alpha e}$ and c'_s were identified for Boom and Ypresian Clays; C_v showed a decrease followed by an increase with increasing σ_v for both soils. This evidenced the competition between the physico-chemical effect and the mechanical effect as identified by Cui et al. (2013) and Nguyen (2013). This also showed that the pore water salt concentration effect prevails only in the region where the hydro-mechanical behavior is dominated by the physico-chemical effect;

(7) The variations of compressibility and swelling capacity parameters showed that the chemical effects stabilized at a certain concentration, and this limit concentration seemed to decrease with increasing active clay minerals like the smectite.

Future characterizations on the pore-water chemical composition effects on the hydro-mechanical behaviours of natural stiff clays, Belgian candidate for host formation of geological radioactive waste disposal, can go further by:

(i) applying a more severe criterion of pore-water replacement, for example, by collecting and measuring electrical conductivity of the expulsed water at the outlet upon injection phase, instead of a simple volumic criterion at the inlet as in the present study;

(ii) applying a better load path with smaller loading/unloading steps around the swelling (threshold) stress σ_s, so that chemical effect on the swelling stress could be investigated without doing separated swelling tests;

(iii) testing Ypresian Clays with distilled water and lower salt concentrations, as for Boom Clay in the present study, to fully investigate chemical effect on this formation. On the

other side, higher salt concentrations (> 30 g/L) should tested as well on both formations to confirm the stabilizing concentration of chemical effects on the hydro-mechanical behaviours, and thus give a more complete information to the end-users on the variation ranges of the hydro-mechanical parameters under these effects for short- and long-term safety assessements.

6. References

AFNOR, 1992. Sols: reconnaissance et essai. Analyse granulométrique des sols. Méthode par sédimentation.

AFNOR, 1997. Sols: reconnaissance et essais. Essais œdométriques. Partie 1: Essai de compressibilité sur matériaux fins quasi saturés avec chargement par paliers.

ASTM, 2006. Standard Practice for Classification of Soils for Engineering Purposes (Unified Soil Classification System) D 2487 - 06.

Baldi, G., Hueckel, T., Pellegrini, R., 1988. Thermal volume changes of the mineral-water system in low-porosity clay soils. Canadian geotechnical journal 25, 807–825.

Burland, J.B., 1990. On the compressibiity and shear strength of natural clays. Géotechnique 40, 329–378.

Cammaer, C., Cockaerts, G., Schiltz, M., 2009. Drilling and géological report ON-KALLO-1, ON-KALLO-2, ON-KALLO-3 (No. Samsuffit R2009-01). ONDRAF/NIRAS.

Carrier, W.D., 1985. Consolidation Parameters Derived From Index Tests. Geotechnique 35, 211–213.

Castellanos, E., Villar, M.V., Romero, E., Lloret, A., Gens, A., 2008. Chemical impact on the hydro-mechanical behaviour of high-density FEBEX bentonite. Physics and Chemistry of the Earth 33, S516–S526.

Chapman, D.L., 1913. A contribution to the theory of electrocapillarity. Philosophical Magazine 25, 475–481.

Chen, J., Anandarajah, A., Inyang, H., 2000. Pore fluid properties and compressibility of kaolinite. Journal of geotechnical and geoenvironmental engineering 126, 798–807.

Coll, C., 2005. Endommagement des roches argileuses et perméabilité induite au voisinage d'ouvrage souterrains. Université Joseph Fourier-Grenoble 1, Grenoble.

Coll, C., Collin, F., Radu, J.P., Illing, P., Schroeder, C., Charlier, R., 2008. Longterm behavior of Boom Clay. Influence of clay viscosity on the far field pore pressure distribution. ULg.

Cui, Y.J., Yahia-Aissa, M. and Delage, P., 2002. A model for the volume change behaviour of heavily compacted swelling clays. Engineering Geology 64 (2-3), 233-250.

Cui, Y.J., Delage, P., Alzoghbi, P., 2003. Retention and transport of a hydrocarbon in a silt. Géotechnique 53, 83–91.

Cui, Y.J., Nguyen, X.P., Tang, A.M., Li, X.L., 2013. An insight into the unloading/reloading loops on the compression curve of saturated clays. Applied Clay Science. Accepted for publication.

Daupley, X., 1997. Etude du potentiel de l'eau interstitielle d'une roche argileuse et de relations entre ses propriétés hydriques et mécaniques. Application aux argilites de Torcien de la région de Tournemire. Ecole Nationale Supérieure des Mines de Paris, Géologie de l'Ingénieur.

De Craen, M., Wang, L., van Geet, M., Moors, H., 2004. Geochemistry of Boom Clay pore water at the Mol site - Status 2004 (Scientific report No. SCK•CEN-BLG-990-04/MDC/P-48). SCK•CEN, Waste & Disposal Department, Boeretang 200, 2400 Mol, Belgium.

De Craen, M., Wemaere, I., Labat, S., van Geet, M., 2006. Geochemical analyses of Boom Clay pore water and underlying aquifers in the Essen-1 borehole (No. SCK•CEN-ER-19. 06/MDC/P-47). SCK•CEN.

Delage, P., Marcial, D., Cui, Y.J., Ruiz, X. (2006). Ageing effects in a compacted bentonite: A microstructure approach, Géotechnique 56 (5), 291-304.

Delage, P., Le, T. T., Tang, A. M., Cui, Y. J. & Li, X. L. (2007), 'Suction effects in deep boom clay block samples', Géotechnique 57 (1), 239–244.

Deng, Y.F., Cui, Y.J., Tang, A.M., Nguyen, X.P., Li, X.L., van Geet, M., 2011a. Investigating the pore-water chemistry effects on the volume change behaviour of Boom clay. Physics and Chemistry of the Earth 36, 1905 – 1912.

Deng, Y.F., Tang, A.M., Cui, Y.J., Nguyen, X.P., Li, X.L., Wouters, L., 2011b. Laboratory hydro-mechanical characterisation of Boom Clay at Essen and Mol. Physics and Chemistry of the Earth 36, 1878 – 1890.

Deng, Y.F., Tang, A.M., Cui, Y.J., Li, X.L., 2011c. Study on the hydraulic conductivity of Boom clay. Canadian Geotechnical Journal 48, 1491–1470.

Deng, Y.F., Cui, Y.J., Tang, A.M., Li, X.L., Sillen, X., 2012. An experimental study on the secondary deformation of Boom Clay. Applied Clay Science 59-60, 19-25.

Di Maio, C., 1996. Exposure of bentonite to salt solution: osmotic and mechanical effects. Géotechnique 46, 695–707.

Di Maio, C., 1998. Discussion: Exposure of bentonite to salt solution: osmotic and mechanical effects. Di Maio, C., 1996. Géotechnique 46 (4), 695-707. Géotechnique 48, 433–436.

Di Maio, C., Fenelli, G.B., 1994. Residual strength of kaolin and bentonite: the influence of their constituent pore fluid. Géotechnique 44, 211–226.

Di Maio, C., Santoli, L., Schiavone, P., 2004. Volume change behavior of clays: the influence of mineral composition, pore fluid composition and stress state. Mechanics of Materials 36, 435–451.

Fernandez, F., Quigley, R.M., 1985. Hydraulic conductivity of natural clays permeated with

simple liquid hydrocarbons. Canadian Geotechnical Journal 22, 205–214.

Gajo, A., Loret, B., 2007. The mechanics of active clays circulated by salts, acids and bases. Journal of the Mechanics and Physics of Solids 55, 1762–1801.

Gajo, A., Maines, M., 2007. Mechanical effects of aqueous solutions of inorganic acids and bases on a natural active clay. Géotechnique 57, 687–699.

Gouy, G., 1910. Sur la constitution de la charge electrique a la surface d'un electrolyte. Anniue Physique (Paris) 9, 457–468.

Karnland, O., Pusch, R., Sandén, T., 1992. The importance of electrolyte on the physical properties of MX-80 bentonite (No. Report AR 92-35). SKB, Stockholm (in Swedish).

Le, T.T., Cui, Y.J., Munoz, J.J., Delage, P., Tang, A.M., Li, X.L., 2011. Studying the stress-suction coupling in soils using an œdometer equipped with a high capacity tensiometer. Front. Archit. Civ. Eng.China, 5(2), 160–170.

Lima, A., 2011. Themo-Hydro-Mechanical behaviour of two deep Belgian clay formations: Boom and Ypresian clays. Universitat Politècnica de Catalunya, Spain.

Loret, B., Hueckel, T., Gajo, A., 2002. Chemo-mechanical coupling in saturated porous media: elastic–plastic behaviour of homoionic expansive clays. International Journal of Solids and Structures 39, 2773–2806.

Mitchell, J.K., Soga, K., 2005. Fundamentals of soil behavior. John Wiley & Sons, Inc.

Mokni, N., Romero, E., Olivella, S., 2012. Joint effect of osmotic and matric suction on hydro-mechanical behavior of Boom Clay. Presented at the Clay in natural and engineered barriers for radioactif waste confinement. 5th international meeting, Montpellier.

Musso, G., Romero, E., Vecchia, G.D., 2013. Double-structure effects on the chemo-hydro-mechanical behaviour of a compacted active clay. Géotechnique 63, 206–220.

Nguyen, X.P., 2013. Étude du comportement chimico-hydro-mécanique des argiles raides dans le contexte du stockage géologique de déchets radioactifs. Ecole des Ponts ParisTech.

Olson, R.O., Mesri, G., 1970. Mechanisms controlling compressibility of clays. Journal of Soil Mechanics and Foundation Division, Proceeding of the American Society of Civil Engineers 6, 1863–1878.

ONDRAF, 2001. Safety Assessment and Feasibility Interim Report 2 (No. SAFIR2). ONDRAF.

Push, R., 2001. Experimental study of the effect of high porewater salinity on the physical properties of a natural smectitic clay (No. Technical Report TR-01-07). SKB, Stockholm.

Raju, N.P.S.R., Pandian, N.S., Nagaraj, T.S., 1995. Analysis and Estimation of Coefficient of Consolidation. Geotechnical Testing Jounal 18, 252–258.

Rao, S.M., Thyagaraj, T., 2007. Swell-compression behavior of compacted clays under chemical gradients. Canadian Geotechnical Journal 44, 520–532.

Robinson, R.G., Allam, M.M., 1998. Effect of clay mineralogy on coefficient of consolidation. Clays and Clay Minerals 46, 596–600.

Rolfe, P.F., Aylmore, L.A.G., 1977. Water and salt flow through compacted clays: I. Permeability of compacted illite and montmorillonite. Soil Science Society of America Journal

41, 489–495.

Romero, M.E., 1999. Characterisation and thermo-hydro-mechanical behaviour of unsaturated Boom clay: an experimental study. Universitat Politècnica de Catalunya.

Sridharan, A., Nagaraj, B., 2004. Coefficient of Consolidation and its Correlation with Index Properties of Remolded Soils. Geotechnical Testing Jounal 27, 1–6.

Sridharan, A., Rao, G.V., 1973. Mechanisms controlling volume change of saturated clays and the role of the effective stress concept. Géotechnique 23, 359–382.

Studds, P.G., Stewart, D.I., Cousens, T.W., 1998. The effects of salt solutions on the properties of bentonite–sand mixtures. Clay Minerals 33, 651–660.

van Marcke, P., 2009. Existing information on the Ypresian clays, in: Meeting on the THMC Characterisation of Ypresian Clays.

van Marcke, P., Laenen, B., 2005. The Ypresian clay as possible host rock for radioactive waste disposal: An evaluation. ONDRAF.

Vandenberghe, N. (2011), Qualitative & quantitative mineralogical analyses of ypresian clay, Technical report, KU Leuven.

Villar, M.V., 2005. MX-80 bentonite. Thermo-hydro-mechanical characterisation performed at CIEMAT in the context of the prototype project. (No. Informes Técnicos 1053). CIEMAT, Madrid.

Wahid, A.S., Gajo, A., Di Maggio, R., 2011a. Chemo-mechanical effects in kaolinite. Part 1: prepared samples. Géotechnique 61, 439–447.

Wahid, A.S., Gajo, A., Di Maggio, R., 2011b. Chemo-mechanical effects in kaolinite. Part 2: exposed samples and chemical and phase analyses. Géotechnique 61, 449–457.

Wakim, J., 2005. Influence des solutions aqueuses sur le comportement mécanique des roches argileuses. Ecole Nationale Supérieure des Mines de Paris.

Wang, P., Anderko, A., 2001. Computation of dielectric constants of solvent mixtures and electrolyte solution. Fluid phase equilibria 186, 203–122.

Yukselen-Aksoy, Y., Kaya, A., Ören, A. H., 2008. Seawater effect on consistency limits and compressibility characteristics of clays. Engineering Geology 102, 54–61.

List of Tables

Table 1: Mineralogical compositions in Boom (BE83) and Ypresian (YK74) Clays

Table 2: Mineralogical composition in the clay fractions (fraction < 2 μm)

Table 3: Physical and index properties of Boom and Ypresian Clays

Table 4: Pore-water chemical compositions for Boom and Ypresian Clays

Table 5: Test program

List of Figures

Figure 1: Particle-size distribution curves of Boom and Ypresian Clays

Figure 2: Typical loading procedure

Figure 3: Compression curve of test BO4 (Boom Clay, NaCl solution at 30 g/L-concentration)

Figure 4: Consolidation curve for the last loading step before soaking, soaking and injection of NaCl solution at 30 g/L-concentration in test BO4 (Boom Clay)

Figure 5: Void ratio (a) and injection pressure (b) changes during the injection phase in test BO4 (Boom Clay, NaCl solution at 30 g/L-concentration)

Figure 6: Chemically induced volume change versus pore water Na^+ concentration during solution injection

Figure 7: Variations of swelling (a) and compression (b) slopes with vertical stress

Figure 8: Variations of œdometric modulus with vertical stress during unloading I-II (a) and reloading II-III (b)

Figure 9: Variations of consolidation coefficient with a) void ratio and b) vertical stress during reloading

Figure 10: Variations of secondary compression/swelling coefficient with void ratio for Boom Clay and Ypresian Clays

Figure 11: Correlations between $C_{\alpha e}$ and c'_c or c'_s for Boom Clay and Ypresian Clays

Figure 12: Variations of intrinsic permeability with void ratio

Figure 13: Results of MIP tests on Boom Clay: (a) cumulative curves, (b) derived curves

Figure 14: Results of MIP tests on Ypresian Clays: (a) cumulative curves, (b) derived curves

Figure 15: SEM photos of Boom Clay samples on the section perpendicular to bedding plane (marked by black lines)

Figure 16: SEM images of Ypresian Clays samples on the section perpendicular to the bedding plane (marked by black lines)

Figure 17: Threshold stress σ_s

Table 1: Mineralogical compositions in Boom (BE83) and Ypresian (YK74) Clays

Minerals (wt %)	BE83[(1)]	YK74[(2)]
Clays	40	57
Illite	10	5
Kaolinite	30	3
Smectite		33
Illite/Smectite		12
Chlorite (or others)		4
Non clays	60	43
Quartz	60	31
Dolomite		0.8
Pyrite	Trace	0.4
K-feldspar	Trace	6
Plagioclase		5

Table 2: Mineralogical composition in the clay fractions (fraction < 2 µm)

Minerals (wt %)	BE83[(1)]	YK74[(2)]
Illite	20	10
Smectite	20	63
Illite/Smectite	20	22
Kaolinite	35	2
Others	5	3

(1): Deng et al. (2011a, 2011b, 2011c, 2012) and Nguyen (2013)

(2): Vandenberghe (2011)

Table 3: Physical and index properties of Boom and Ypresian Clays

Core	Depth (m)	G_s (-)	LL (-)	PL (-)	PI (-)	VBS (g/100g)	$CaCO_3$ (%wt)	e_0 (-)	w_0 (%)	S_{r0} (%)	ρ_0 (Mg/m^3)
BE83[(1)]	226.65 - 227.65	2.64	67.2	32.5	34.7	6.7	0.76	0.69 - 0.72	26.20 - 28.13	98.72 - 100	1.95 - 1.97
YK74	361.81 - 362.60	2.80	136.6	36.1	100.5	13.1	0.88	0.84	28.34 - 28.52	90.95 - 95.27	1.92 - 1.96

(1): Deng et al. (2011a, 2011b, 2011c, 2012) and Nguyen (2013).

G_s: Specific gravity; LL: liquid limit; PL: plastic limit; PI: plasticity index, VBS: blue methylene value; $CaCO_3$: carbonates content, e_0: initial void ratio; w_0: initial water content; S_{r0}: initial degree of saturation; ρ_0: initial density.

Table 4: Pore-water chemical compositions for Boom and Ypresian Clays

Salts	Concentration (10^{-3} M)		Concentration (g/L)	
	BE83[(1)]	YK74[(2)]	BE83[(1)]	YK74[(2)]
NaCl	54.6	117.9	3.195	6.896
Na_2SO_4	5.2	6.3	0.742	0.896
$NaHCO_3$	7.2		0.602	
KCl	0.6		0.046	
$CaCl_2$	0.5		0.058	
$MgCl_2$	1.4		0.137	
Salinity			4.78	7.79
Total Na+	72.2	130.5		

(1): De Craen et al. (2006)

(2): van Marcke (2009)

Table 5: Test program

Soils	Test ID	Solution soaked	Solution injected at 1 MPa	e_0 (-)	S_{r0} (%)
Boom Clay	BO1[(1)]	SBCW	H2O	0.730	-
	BO2[(1)]	SBCW	SBCW	0.730	-
	BO3	SBCW	NaCl 15 g/L	0.720	99.09
	BO4	SBCW	NaCl 30 g/L	0.723	98.72
Ypresian Clays	YO1	SYCW[(2)]	NaCl 15 g/L	0.840	94.57
	YO2	SYCW	NaCl 30 g/L	0.839	95.27

(1): Deng et al. (2011a) and Nguyen (2013)

(2): Synthetic Ypresian Clay Water

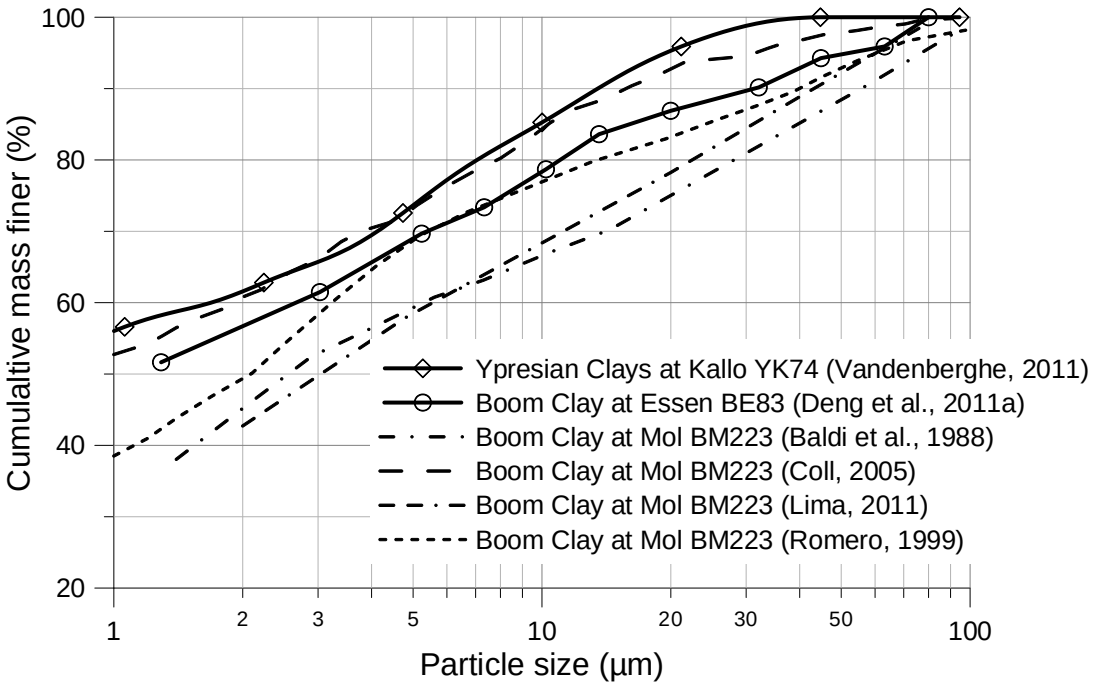

Figure 1: Particle-size distribution curves of Boom and Ypresian Clays

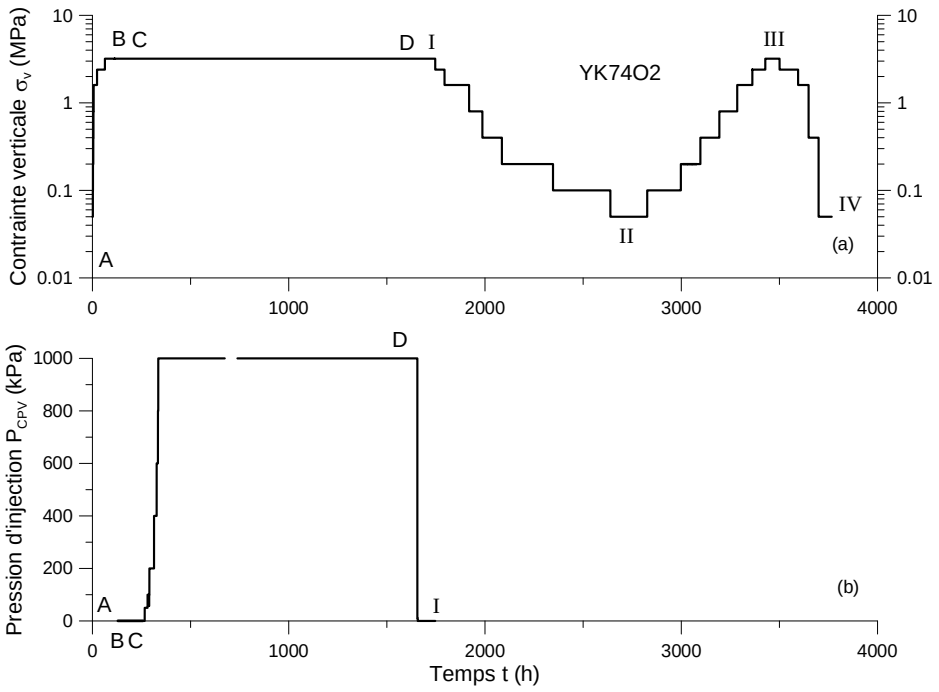

Figure 2: Typical loading procedure

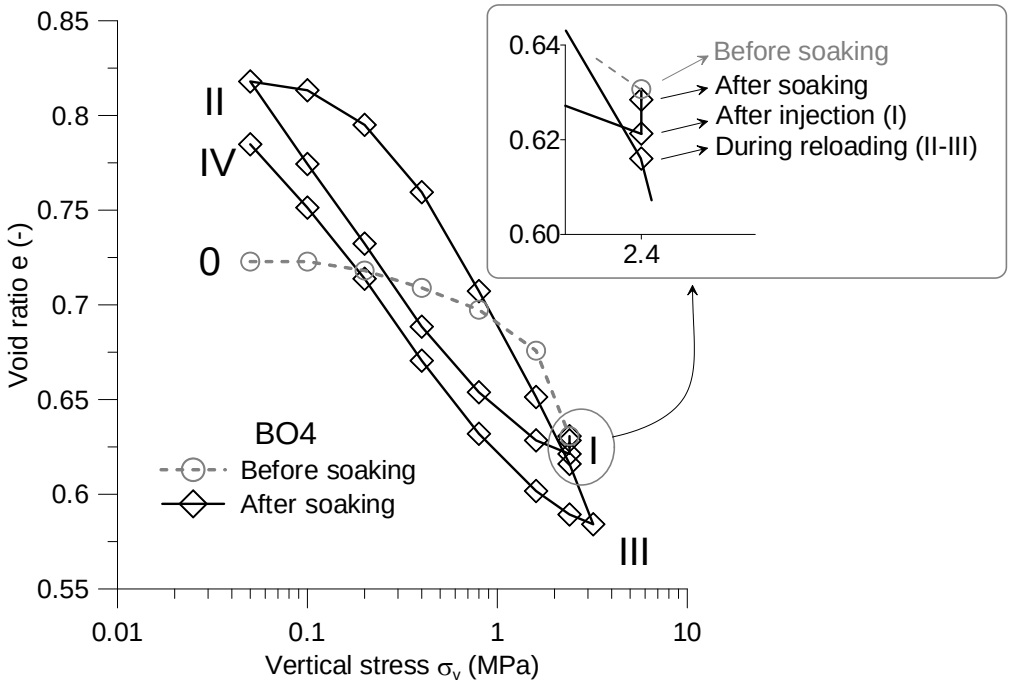

Figure 3: Compression curve of test BO4 (Boom Clay, NaCl solution at 30 g/L-concentration)

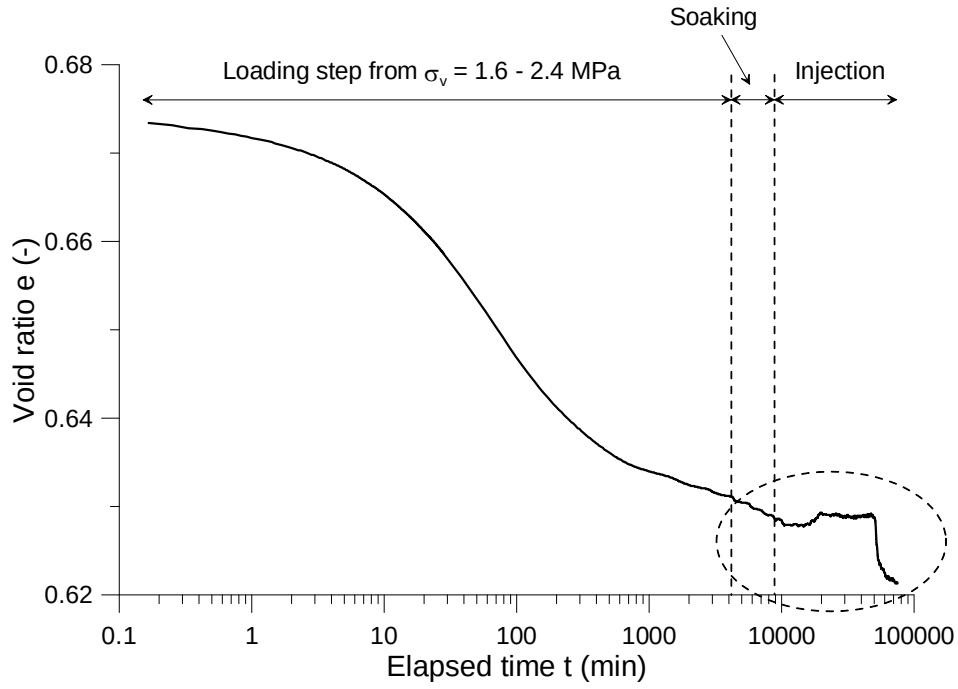

Figure 4: Consolidation curve for the last loading step before soaking, soaking and injection of NaCl solution at 30 g/L-concentration in test BO4 (Boom Clay)

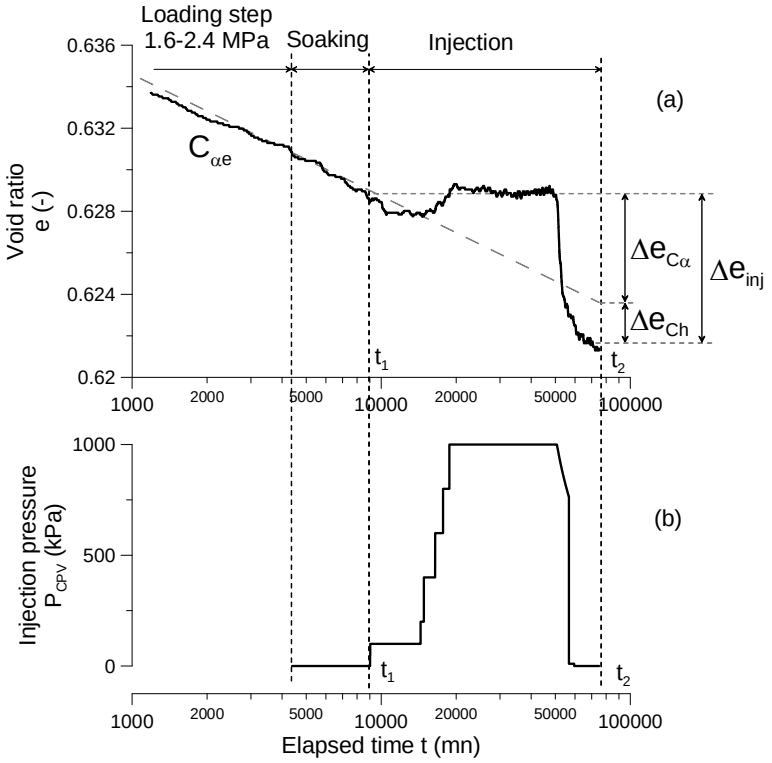

Figure 5: Void ratio (a) and injection pressure (b) changes during the injection phase in test BO4 (Boom Clay, NaCl solution at 30 g/L-concentration)

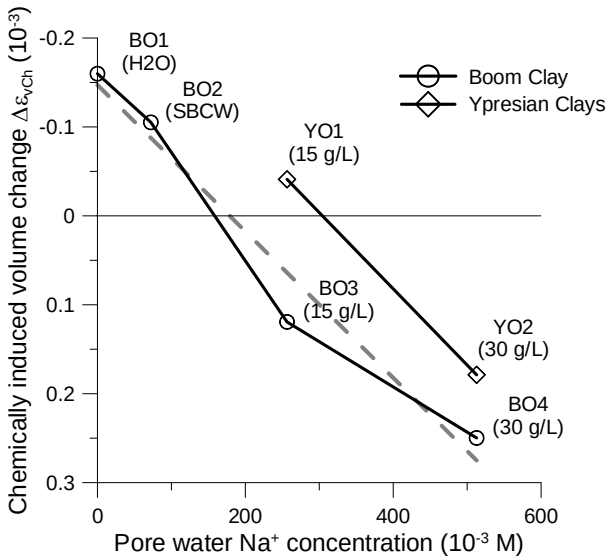

Figure 6: Chemically induced volume change versus pore water Na^+ concentration during solution injection

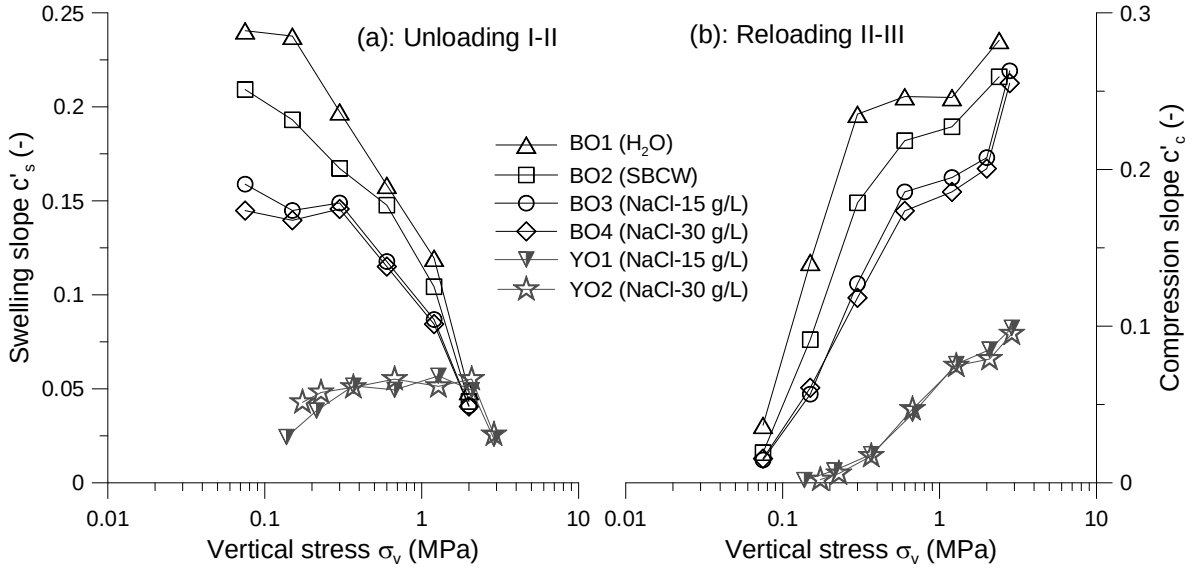

Figure 7: Variations of swelling (a) and compression (b) slopes with vertical stress

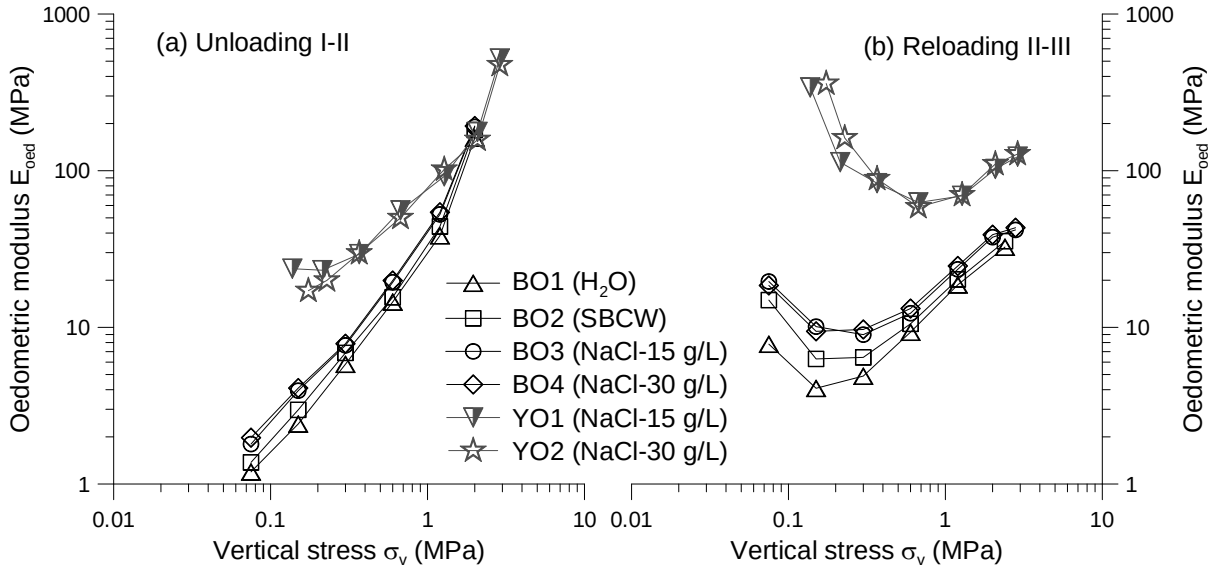

Figure 8: Variations of œdometric modulus with vertical stress during unloading I-II (a) and reloading II-III (b)

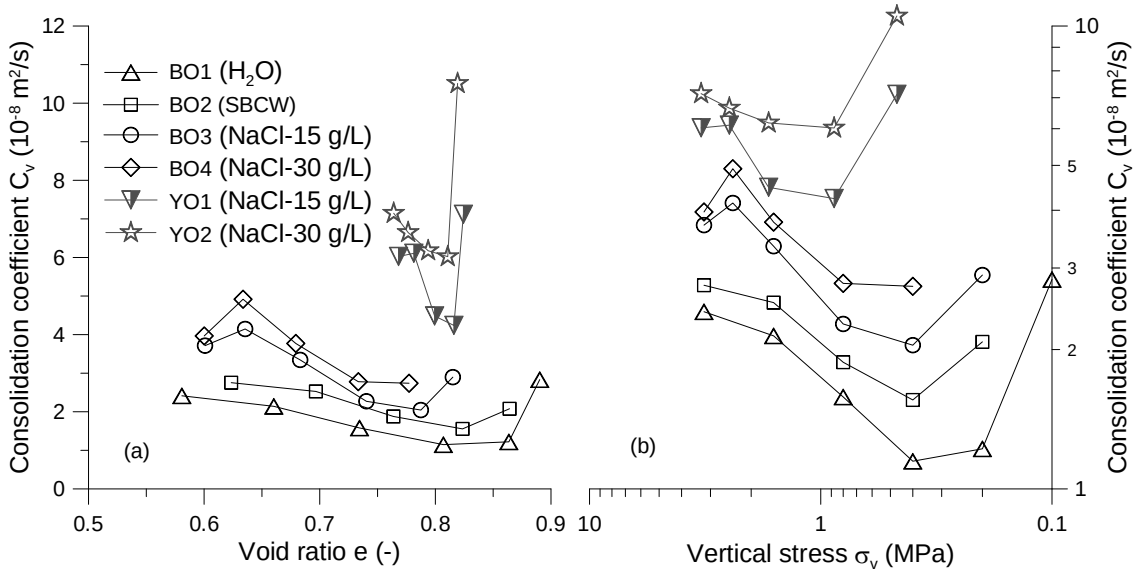

Figure 9: Variations of consolidation coefficient with a) void ratio and b) vertical stress during reloading

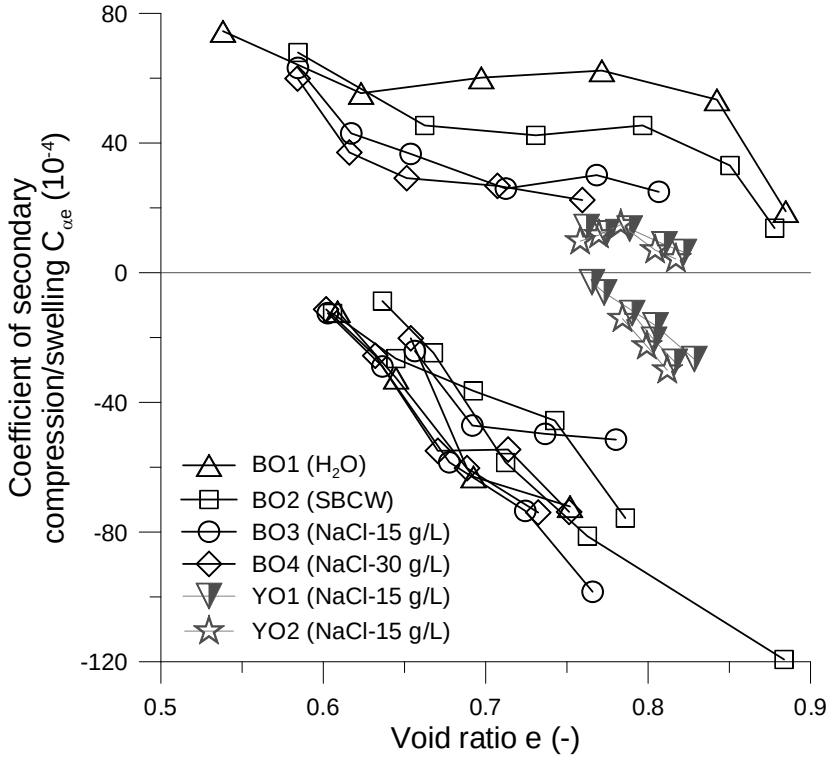

Figure 10: Variations of secondary compression/swelling coefficient with void ratio for Boom Clay and Ypresian Clays

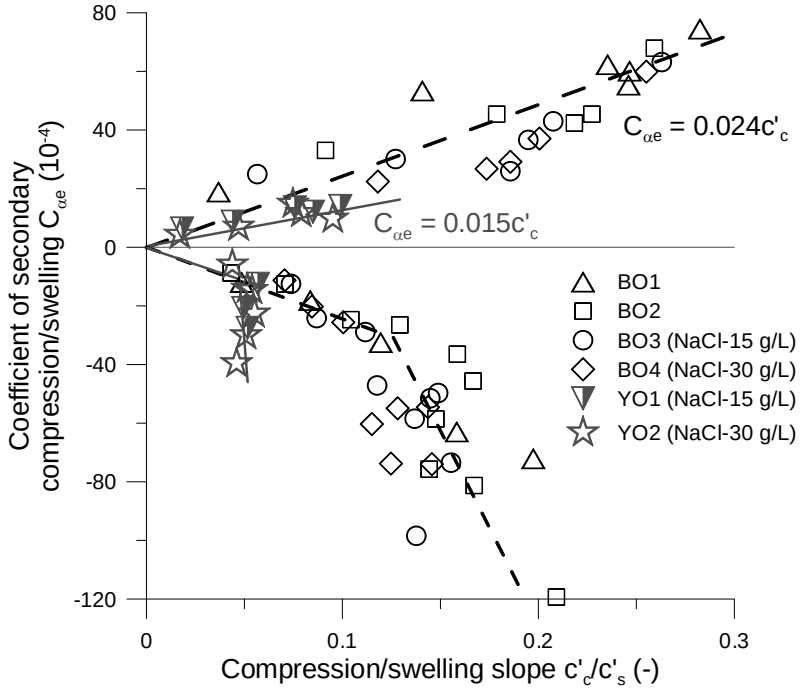

Figure 11: Correlations between $C_{\alpha e}$ and c'_c or c'_s for Boom Clay and Ypresian Clays

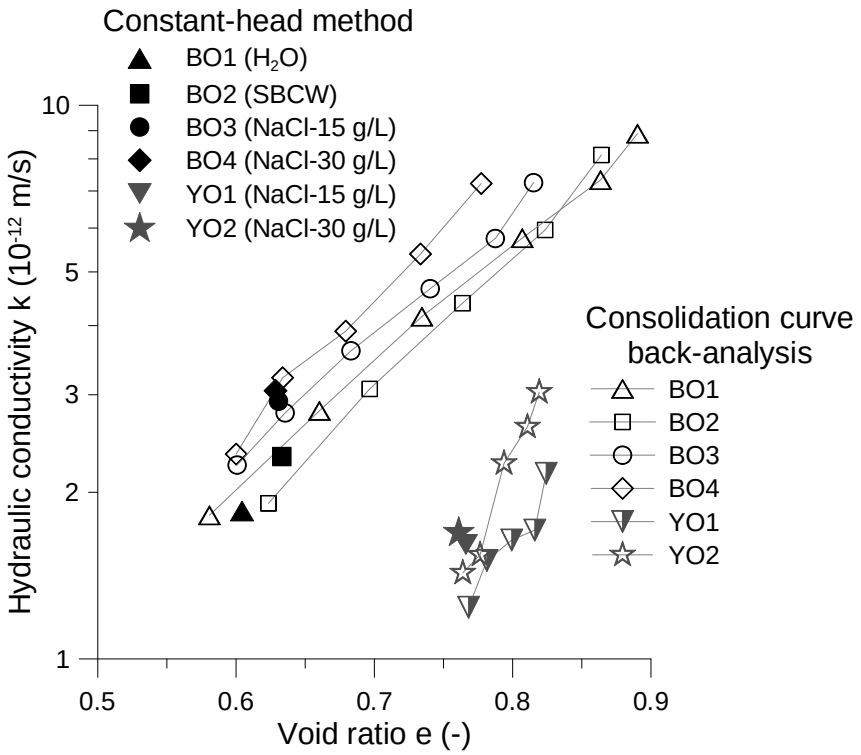

Figure 12: Variations of intrinsic permeability with void ratio

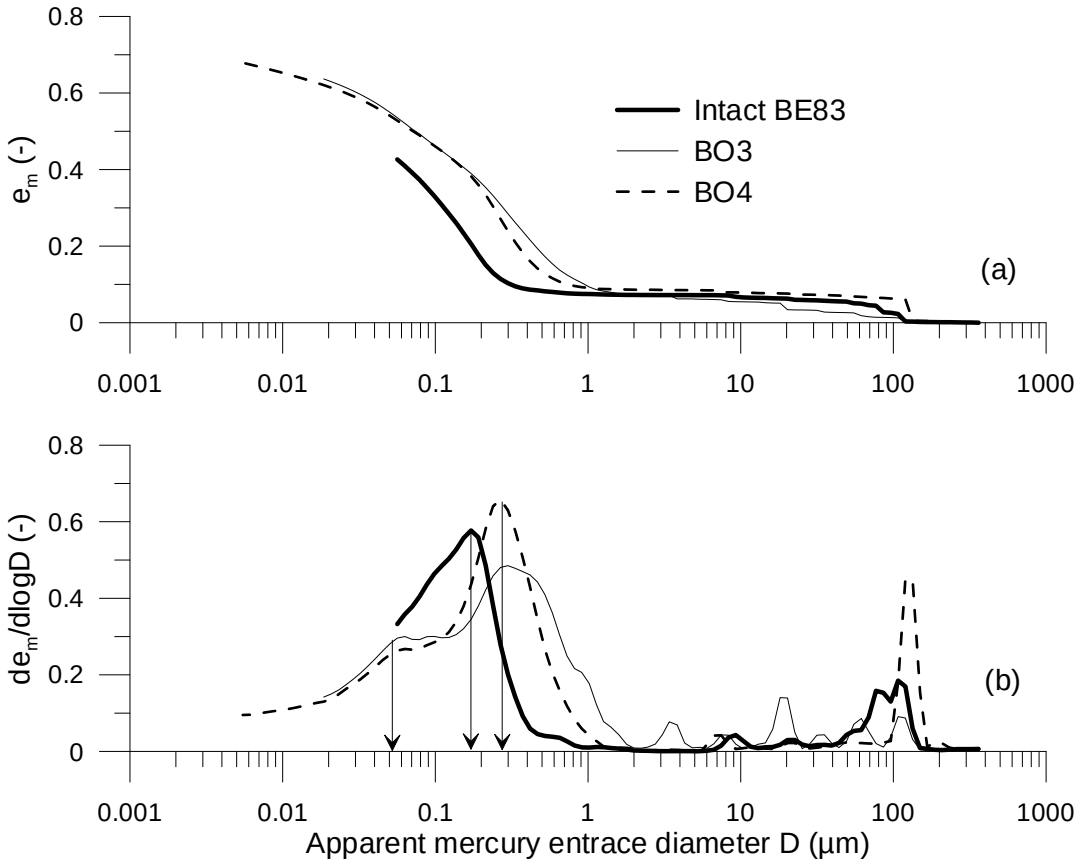

Figure 13: Results of MIP tests on Boom Clay: (a) cumulative curves, (b) derived curves

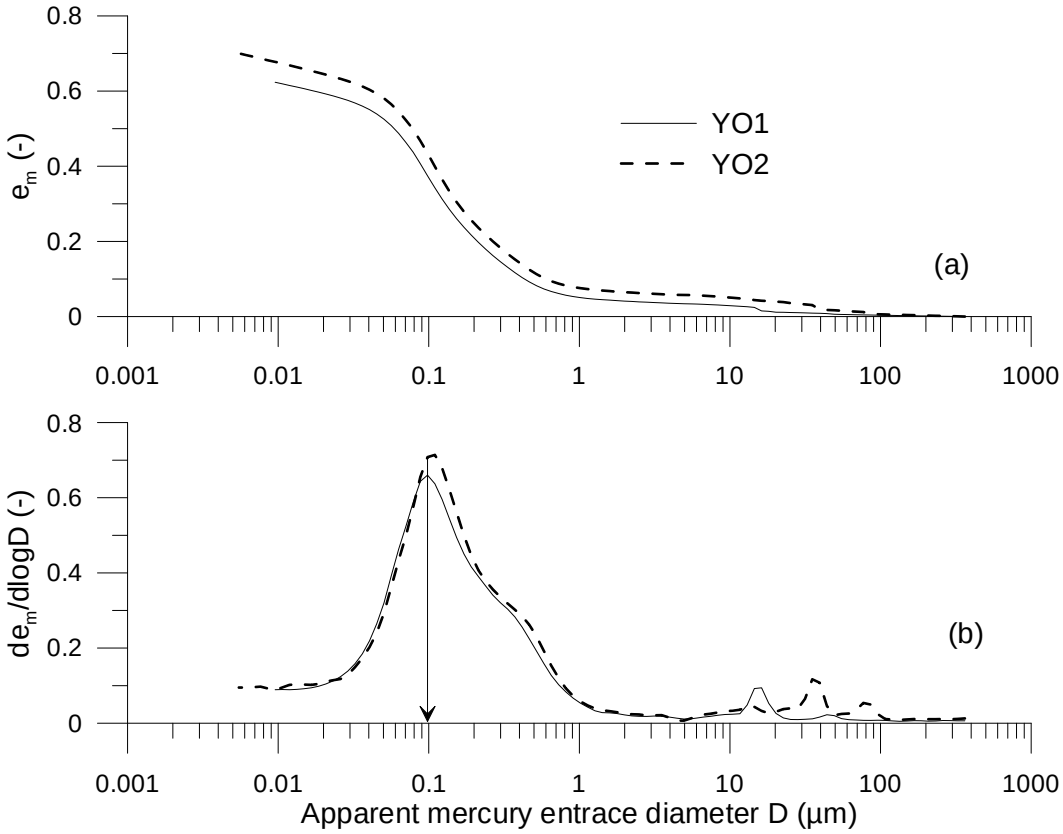

Figure 14: Results of MIP tests on Ypresian Clays: (a) cumulative curves, (b) derived curves

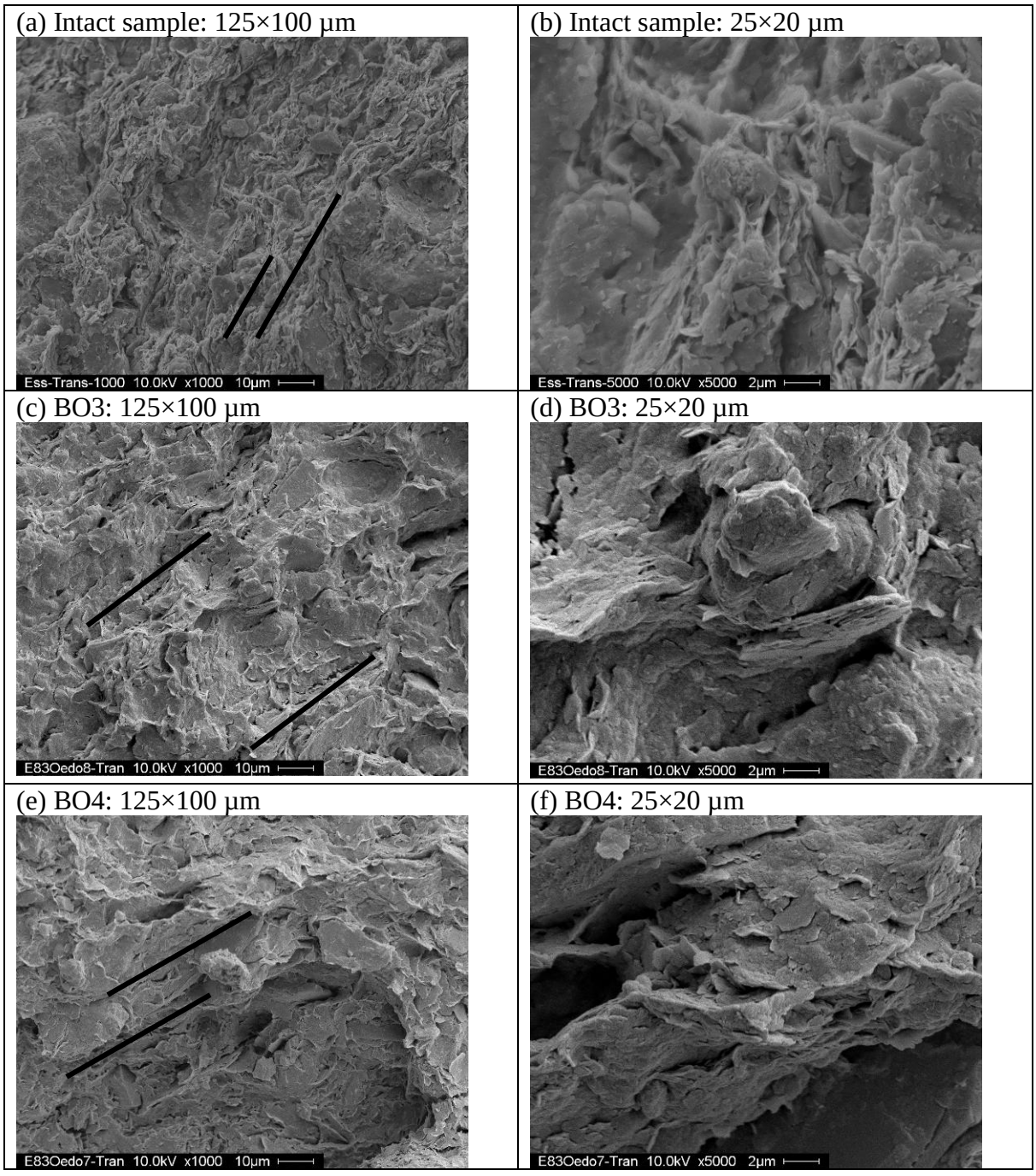

Figure 15: SEM photos of Boom Clay samples on the section perpendicular to bedding plane (marked by black lines)

(a) YO1: 125×100 µm

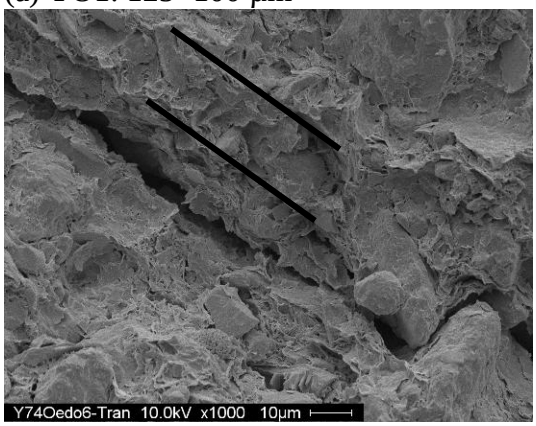

(b) YO1: 25×20 µm

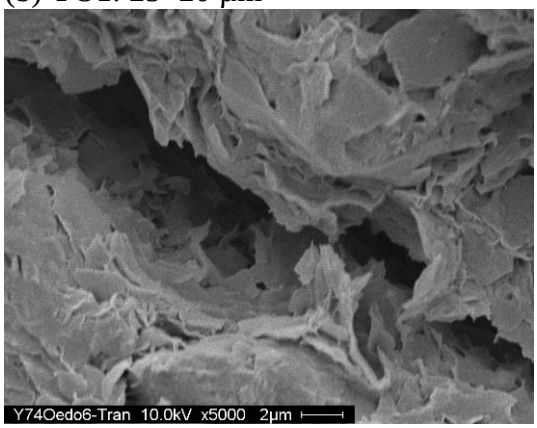

(c) YO2: 250×200 µm

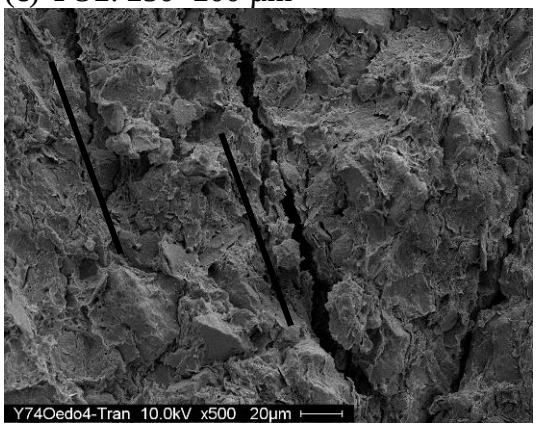

(d) YO2: 62.5×50 µm

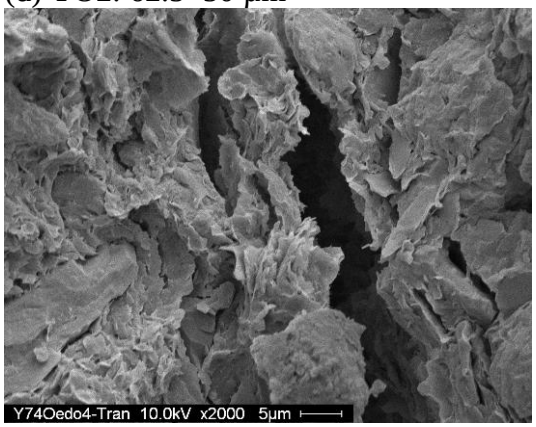

Figure 16: SEM images of Ypresian Clays samples on the section perpendicular to the bedding plane (marked by black lines)

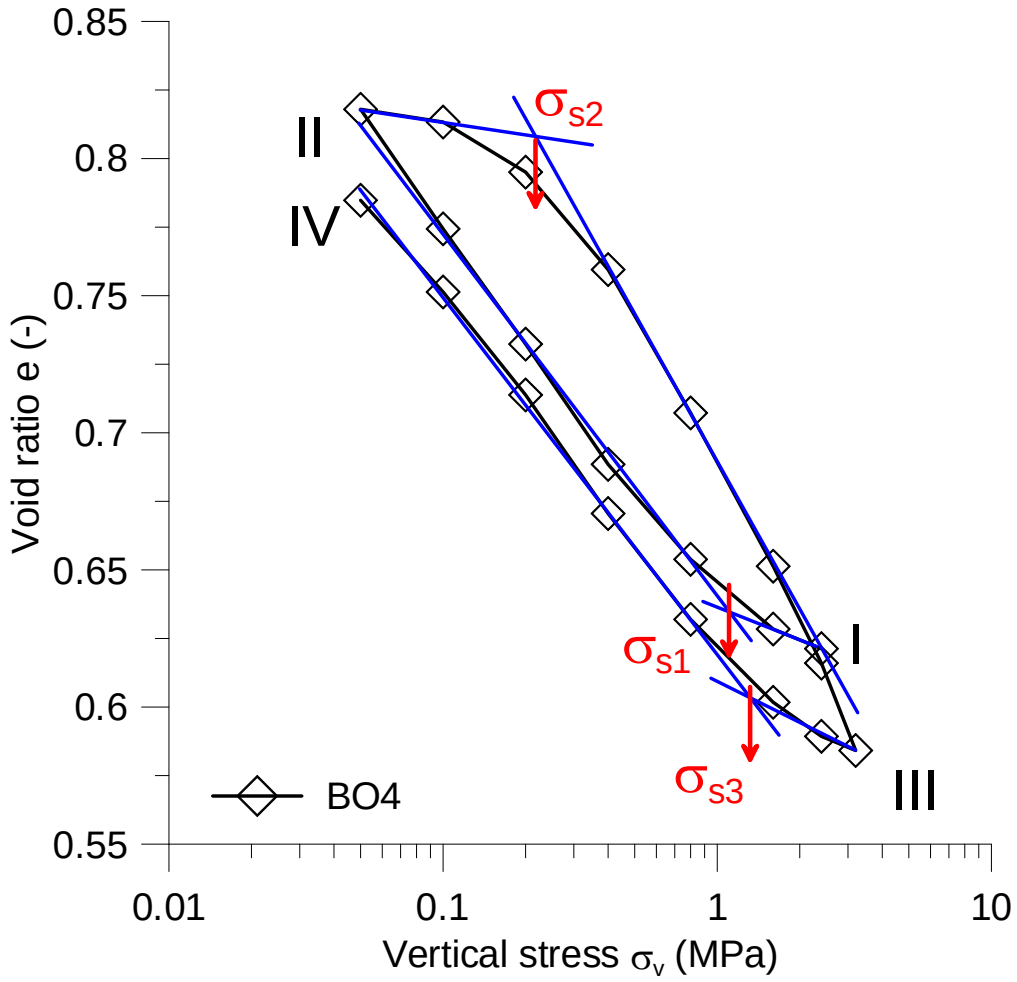

Figure 17: Threshold stress σ_s